Electronic Supplementary Information

Biphenyl end-capped bithiazole co-oligomers for high performance organic thin film field effect transistors

Kazuaki Oniwa,[a] Hiromasa Kikuchi,[a] Thangavel Kanagasekaran,[a] Hidekazu Shimotani,[b] Susumu Ikeda,[a] Naoki Asao,[a] Yoshinori Yamamoto,[a,c] Katsumi Tanigaki[a,b] and Tienan Jin*[a]

[a] WPI-Advanced Institute for Materials Research (WPI-AIMR), Tohoku University, Sendai 980-8577, Japan. Fax: +81-22-217-5979; Tel: +81-22-217-6177; E-mail: tjin@m.tohoku.ac.jp

[b] Graduate School of Science, Department of Physics, Sendai 980-8578, Tohoku University, Japan.

[c] State Key Laboratory of Fine Chemicals, Dalian University of Technology, Dalian 116012, China.

General Information

The commercially available compounds and solvent were used as received. ^{1}H NMR and ^{13}C NMR spectra were recorded on JEOL JNM AL 400 (400 MHz) spectrometers. ^{1}H NMR spectra are reported as follows: chemical shift in ppm δ relative to the chemical shift of $CDCl_3$ at 7.26 ppm, integration, multiplicities (s = singlet, d = doublet, t = triplet, q = quartet, m = multiplet, and br = broadened), and coupling constants (Hz). ^{13}C NMR spectra were recorded on JEOL JNM AL 400 (100.5 MHz) spectrometers with complete proton decoupling, and chemical shift reported in ppm δ relative to the central line of triplet for $CDCl_3$ at 77 ppm. Scanning electron microscope (SEM) observation was carried out using a JEOL JSM-6500F instrument operated at an accelerating voltage of 30 kV. UV/Vis absorption spectra were recorded on a JASCO V-650DS spectrometer. Fluorescence spectra were recorded on a HITACHI F-7000 spectrophotometer and absolute fluorescence quantum yields were measured by a photon-counting method using an integration sphere on a Hamamatsu Photonics C9920-02 spectrometer. Elemental analyses were measured on J-SCIENCE Lab JM-10 and YANAKO YHS-11 in Central Analytical Facility, Institute of Multidisciplinary Research for Advanced Materials, Tohoku University. DSC was measured by a RIGAKU DSC8230 using N_2 atmosphere at a scan rate of 10 K/min. TGA was measured by a RIGAKU TAG8120. X-ray diffractions were measured by RIGAKU Smart Lab 9SW using Cu-Kα radiation and zero dimensional mode Dte/X as high-speed detector. The ionization potential (IP) was measured using the photoelectron spectrometer surface analyser (Riken Keiki, AC-3E). Column chromatography was carried out employing silica gel 60 N (spherical, neutral, 40~100 μm, KANTO Chemical Co.). Analytical thin-layer chromatography (TLC) was performed on 0.2 mm precoated plate Kieselgel 60 F254 (Merck).

Synthesis of 2,2'-bithiazole

A mixture of 2-bromothiazole (32 mmol, 2.88 mL), $Pd(OAc)_2$ (10 mol%, 718 mg), *n*-Bu_4NBr (16 mmol, 5.16 g), and diisopropylethylamine (32 mmol, 5.57 mL) in toluene (12 mL) was stirred for 18 h at 105 °C. The resulting mixture was poured into water and extracted by $CHCl_3$. After concentration, the residue was purified by silica gel chromatography, giving the corresponding 2,2'-bithiazole in 90% (2.43 g) yield as a yellow solid. ^{1}H NMR (400 MHz, $CDCl_3$): δ 7.90 (d, 2H, *J* = 2.8 Hz), 7.45 (d, 2H, *J* = 2.8 Hz); ^{13}C NMR (100 MHz, $CDCl_3$): δ 161.54, 143.80, 120.87.

Synthesis of 5,5'-dibromo-2,2'-bithiazole

A mixture of 2,2'-bithiazole (6 mmol, 1.01 g) and NBS (24 mmol, 4.27 g) in DMF (30 mL) was stirred for 12 h at 60 °C. The resulting mixture was poured into water and extracted by $CHCl_3$. After concentration, the residue was purified by recrystallization using MeOH and $CHCl_3$, giving the corresponding 5,5'-dibromo-2,2'-bithiazole in 95% (1.85 g) yield as a white solid. ^{1}H NMR (400 MHz, $CDCl_3$): δ 7.75 (s, 2H); ^{13}C NMR (100 MHz, $CDCl_3$): δ 161.79, 145.06, 111.95.

Synthesis of 5,5'-di([1,1'-biphenyl]-4-yl)-2,2'-bithiazole [BP2Tz(in)]

A mixture of 5,5'-dibromo-2,2'-bithiazole (2.5 mmol, 815 mg), [1,1'-biphenyl]-4-ylboronic acid (6.25 mmol, 1.24 g), K_3PO_4・nH_2O (2.8 g), $Pd_2(dba)_3$・$CHCl_3$ (5 mol%, 129 mg), and X-phos (20 mol%, 238 mg) in DMF (18 mL) was stirred at 120 °C for 18 h. The mixture was filtered and the resulting residue was washed by water, MeOH, and $CHCl_3$.

After sublimation at 330 °C under high vacuum, **BP2Tz(in)** was obtained as a yellow solid in 40% (470 mg) yield. Anal. calcd for C30H20N2S2: C 76.24, H 4.27, N 5.93, S 13.57; found: C 75.97, H 4.34, N 5.70, S 13.15%.

Synthesis of 2-([1,1'-biphenyl]-4-yl)thiazole

[1,1'-biphenyl]-4-ylboronic acid (12.2 mmol, 2.42 g), $K_3PO_4 \cdot nH_2O$ (6 g), and $Pd(PPh_3)_4$ were dissolved in DMF (20 mL) under nitrogen atmosphere. Then 2-bromothiazole (10.0 mmol, 0.902 mL) was added. The mixture was stirred for overnight at 100 °C. The resulting mixture was poured into water and extracted by $CHCl_3$. After concentration, the residue was purified by silica gel chromatography, giving the corresponding 2-biphenylthiazole in 70% (1.66 g) yield as a white solid. ^{1}H NMR (400 MHz, $CDCl_3$): δ 8.06 (d, 2H. *J* = 8.0 Hz), 7.90 (d, 1H, *J* = 2.8 Hz), 7.69 (d, 2H, *J* = 8.0 Hz), 7.64 (d, 2H, *J* = 8.0 Hz), 7.40 (t, 2H, *J* = 8.0 Hz), 7.38 (t, 1H, *J* = 8.0 Hz), 7.36 (d, 1H, *J* = 2.8 Hz); ^{13}C NMR (100 MHz, $CDCl_3$): δ 167.99, 143.60, 142.71, 140.11, 132.39, 128.82, 127.71, 127.55, 126.96, 118.72.

Synthesis of 2,2'-di([1,1'-biphenyl]-4-yl)-5,5'-bithiazole [BP2Tz(out)]

To a solution of 2-([1,1'-biphenyl]-4-yl)thiazole (2.1 mmol, 577 mg) in anhydrous THF (6 mL) was added bis(2,2,6,6-tetramethylpiperidine) zinc lithium magnesium chloride complex (3.3 mL of a 0.35 M solution in THF) dropwise over 30 min at rt. The reaction mixture was stirred at room temperature for 1 h and then cooled to -40 °C. Chloranil (2.51 mmol, 616 mg) was added portion-wise over 30 min. The reaction mixture was slowly warmed to 0 °C. The mixture was quenched with sat. NH_4Cl solution (3 mL) and filtered. The resulting residue was washed by water, MeOH, and $CHCl_3$. After sublimation at 325 °C, **BP2Tz(out)** was obtained as a yellow solid in 72% (340 mg) yield. Anal. calcd for C30H20N2S2: C 76.24, H 4.27, N 5.93, S 13.57; found: C 76.24, H 4.36, N 5.92, S 13.29%

Thermal analysis

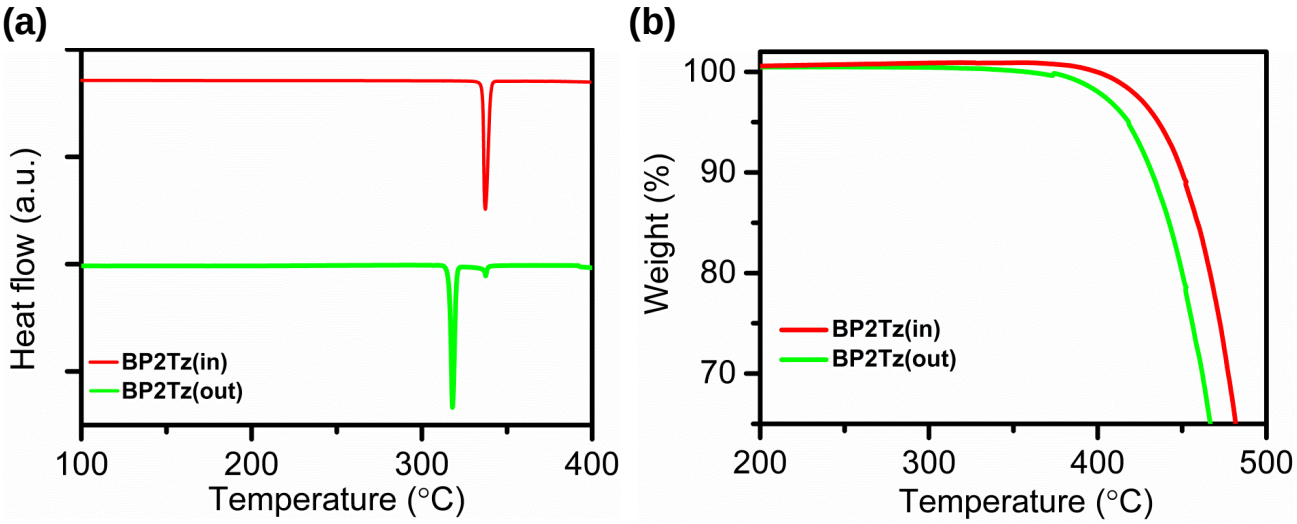

Fig. S1 (a) DSC analysis: melting points: **BP2Tz(in)**: 336 ºC; **BP2Tz(out)**: 318 ºC. (b) TGA analysis: decomposition temperatures (10% loss): **BP2Tz(in)**: 447 ºC; **BP2Tz(out)**: 432 ºC.

Photoelectron yield spectroscopy

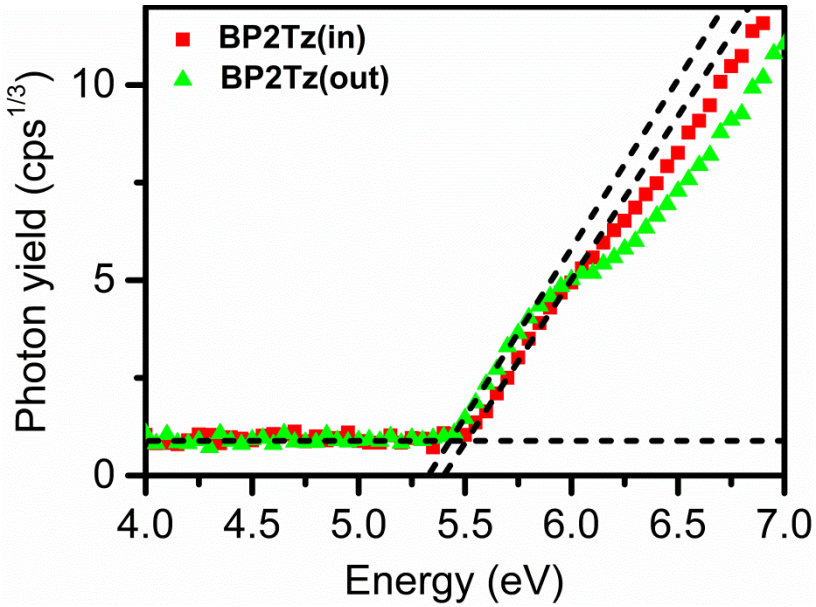

Fig. S2 PYS spectra of **BP2Tz(in)** and **BP2Tz(out)** in thin film state. IP: 5.49 eV for **BP2Tz(in)**, 5.43 eV for **BP2Tz(out)**.

Theoretical calculation of HOMO and LUMO energy levels of BP2Tz series

Computation Details[1]

Calculations of monomer molecule were performed at the DFT level by means of the hybrid B3LYP functional as implemented in Gaussian 09W. The 6-31G++(d, p) basis set was used for the all atoms.

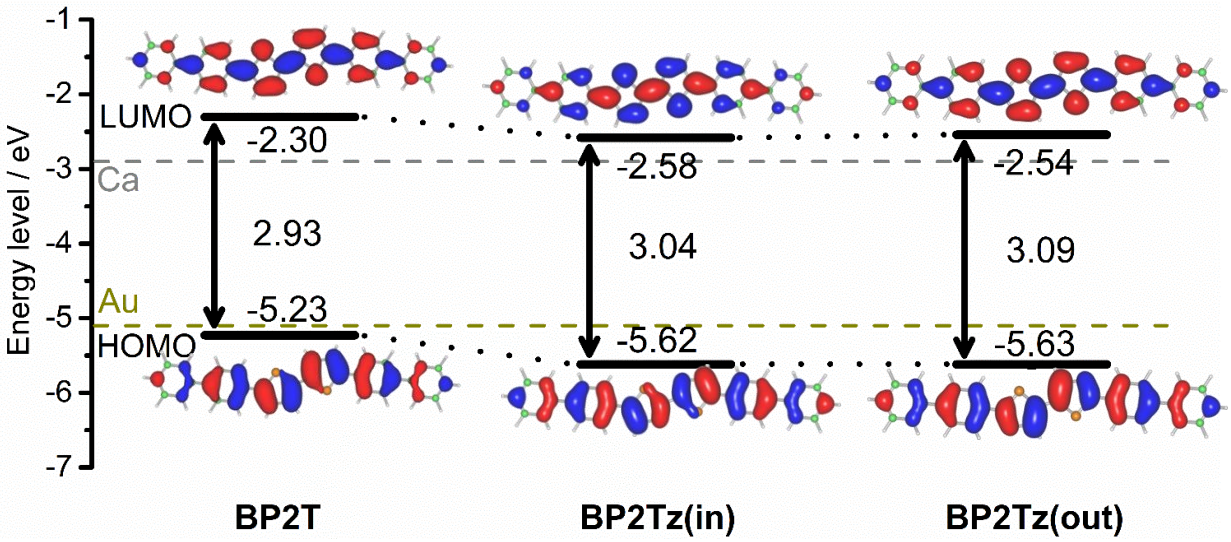

Fig. S3 Energy diagram of theoretical calculated HOMO and LUMO energies with work function of gold and calcium.

Full Computational Details

Cartesian Coordinates and Total Electron Energies

Table S1. BP2Tz(in)

SCF Done: E(RB3LYP) = -2061.2144829

Center Number	Atomic Number	Atomic Type	Coordinates (Angstroms) X	Y	Z
1	6	0	-0.251714	11.764704	0.000000
2	6	0	-1.389383	10.954582	0.000000
3	6	0	-1.268445	9.565226	0.000000
4	6	0	-0.008593	8.933063	0.000000
5	6	0	1.125012	9.770753	0.000000
6	6	0	1.007386	11.160466	0.000000
7	6	0	0.118968	7.447142	0.000000
8	6	0	1.375398	6.807057	0.000000
9	6	0	1.499778	5.423604	0.000000
10	6	0	0.367898	4.585013	0.000000
11	6	0	-0.889459	5.216046	0.000000

12	6	0	-1.007386	6.601681	0.000000
13	6	0	0.507777	3.127977	0.000000
14	6	0	1.663482	2.368061	0.000000
15	6	0	0.242328	0.681032	0.000000
16	16	0	-0.867503	2.041228	0.000000
17	6	0	-0.242328	-0.681032	0.000000
18	6	0	-1.663482	-2.368061	0.000000
19	6	0	-0.507777	-3.127977	0.000000
20	16	0	0.867503	-2.041228	0.000000
21	6	0	-0.367898	-4.585013	0.000000
22	6	0	0.889459	-5.216046	0.000000
23	6	0	1.007386	-6.601681	0.000000
24	6	0	-0.118968	-7.447142	0.000000
25	6	0	-1.375398	-6.807057	0.000000
26	6	0	-1.499778	-5.423604	0.000000
27	6	0	0.008593	-8.933063	0.000000
28	6	0	1.268445	-9.565226	0.000000
29	6	0	1.389383	-10.954582	0.000000
30	6	0	0.251714	-11.764704	0.000000
31	6	0	-1.007386	-11.160466	0.000000
32	6	0	-1.125012	-9.770753	0.000000
33	1	0	-0.344635	12.846564	0.000000
34	1	0	-2.378713	11.403214	0.000000
35	1	0	-2.177702	8.975698	0.000000
36	1	0	2.121631	9.345156	0.000000
37	1	0	1.905715	11.771275	0.000000
38	1	0	2.288111	7.390810	0.000000
39	1	0	2.495743	4.993580	0.000000
40	1	0	-1.796567	4.618638	0.000000
41	1	0	-2.007406	7.018669	0.000000
42	1	0	2.667288	2.774382	0.000000
43	1	0	-2.667288	-2.774382	0.000000
44	1	0	1.796567	-4.618638	0.000000
45	1	0	2.007406	-7.018669	0.000000
46	1	0	-2.288111	-7.390810	0.000000
47	1	0	-2.495743	-4.993580	0.000000
48	1	0	2.177702	-8.975698	0.000000
49	1	0	2.378713	-11.403214	0.000000

50	1	0	0.344635	-12.846564	0.000000
51	1	0	-1.905715	-11.771275	0.000000
52	1	0	-2.121631	-9.345156	0.000000
53	7	0	1.512251	1.013883	0.000000
54	7	0	-1.512251	-1.013883	0.000000

Table S2. BP2Tz(out)

SCF Done: E(RB3LYP) = -2061.2163087

Center Number	Atomic Number	Atomic Type	Coordinates (Angstroms) X	Y	Z
1	6	0	-0.236002	11.772640	0.000000
2	6	0	-1.377853	10.968457	0.000000
3	6	0	-1.263874	9.578529	0.000000
4	6	0	-0.007189	8.939968	0.000000
5	6	0	1.130715	9.771878	0.000000
6	6	0	1.020064	11.162112	0.000000
7	6	0	0.113681	7.453107	0.000000
8	6	0	1.369066	6.809145	0.000000
9	6	0	1.488693	5.425535	0.000000
10	6	0	0.347246	4.603205	0.000000
11	6	0	-0.909852	5.229722	0.000000
12	6	0	-1.020064	6.615768	0.000000
13	6	0	0.505124	3.148530	0.000000
14	6	0	1.518579	1.175928	0.000000
15	6	0	0.228000	0.685073	0.000000
16	16	0	-0.878868	2.043826	0.000000
17	6	0	-0.228000	-0.685073	0.000000
18	6	0	-1.518579	-1.175928	0.000000
19	6	0	-0.505124	-3.148530	0.000000
20	16	0	0.878868	-2.043826	0.000000
21	6	0	-0.347246	-4.603205	0.000000
22	6	0	0.909852	-5.229722	0.000000
23	6	0	1.020064	-6.615768	0.000000
24	6	0	-0.113681	-7.453107	0.000000
25	6	0	-1.369066	-6.809145	0.000000

26	6	0	-1.488693	-5.425535	0.000000
27	6	0	0.007189	-8.939968	0.000000
28	6	0	1.263874	-9.578529	0.000000
29	6	0	1.377853	-10.968457	0.000000
30	6	0	0.236002	-11.772640	0.000000
31	6	0	-1.020064	-11.162112	0.000000
32	6	0	-1.130715	-9.771878	0.000000
33	1	0	-0.323444	12.854966	0.000000
34	1	0	-2.364856	11.422166	0.000000
35	1	0	-2.176242	8.993922	0.000000
36	1	0	2.125005	9.341166	0.000000
37	1	0	1.921444	11.768357	0.000000
38	1	0	2.282943	7.390920	0.000000
39	1	0	2.468372	4.960887	0.000000
40	1	0	-1.819001	4.634698	0.000000
41	1	0	-2.016739	7.040255	0.000000
42	1	0	2.406245	0.553514	0.000000
43	1	0	-2.406245	-0.553514	0.000000
44	1	0	1.819001	-4.634698	0.000000
45	1	0	2.016739	-7.040255	0.000000
46	1	0	-2.282943	-7.390920	0.000000
47	1	0	-2.468372	-4.960887	0.000000
48	1	0	2.176242	-8.993922	0.000000
49	1	0	2.364856	-11.422166	0.000000
50	1	0	0.323444	-12.854966	0.000000
51	1	0	-1.921444	-11.768357	0.000000
52	1	0	-2.125005	-9.341166	0.000000
53	7	0	-1.662023	-2.531124	0.000000
54	7	0	1.662023	2.531124	0.000000

Thin film OFET (OTFT) device fabrication and characterization

Fabrication OTFTs using OTS-treated SiO_2 substrate

A highly doped silicon wafer with a 300 nm thermally grown SiO_2 layer was covered with OTS. These substrates was used in the thin film deposition. Thin film transistors were fabricated by evaporating the highly pure molecules under the high vacuum (10^{-6} Torr) with a thickness of 30 nm, as measured in situ by a quartz crystal microbalance. The thin film deposition rate maintained at 0.1 Å/sec. The top contact symmetric electrodes were deposited by evaporating gold metal through a shadow mask on the top of the thin film. The electrical characterization of thin film transistors were performed in the glove box under an inert Ar atmosphere by using a semiconductor parameter analyzer (Agilent Technology B1500A) and a CCD camera through an optical microscope.

Table S3. OTFTs performances at various substrate temperatures (T_{sub})

Compound	T_{sub} / °C	μ_{max} / $cm^2V^{-1}s^{-1}$	μ_{ave} / $cm^2V^{-1}s^{-1}$	V_{th} / V	*on* / *off*
BP2Tz(in)	40	0.48	0.28	-29	10^5
	60	1.5	1.1	-31	10^6
	80	2.9	2.8	-35	10^6
	100	3.5	3.2	-28	10^8
	120	2.1	1.9	-31	10^6
	140	1.8	1.6	-19	10^6
	160	2.0	1.5	-27	10^7
	180	1.2	0.68	-26	10^5
BP2Tz(out)	40	0.085	0.075	-44	10^4
	60	0.17	0.13	9	10^5
	80	0.30	0.26	-5	10^5
	100	0.44	0.40	-19	10^5
	120	0.36	0.32	-15	10^7
	140	0.32	0.27	-1	10^5
	160	0.50	0.32	-31	10^7
	180	0.15	0.13	-54	10^5

Scanning electron microscopy (SEM) image

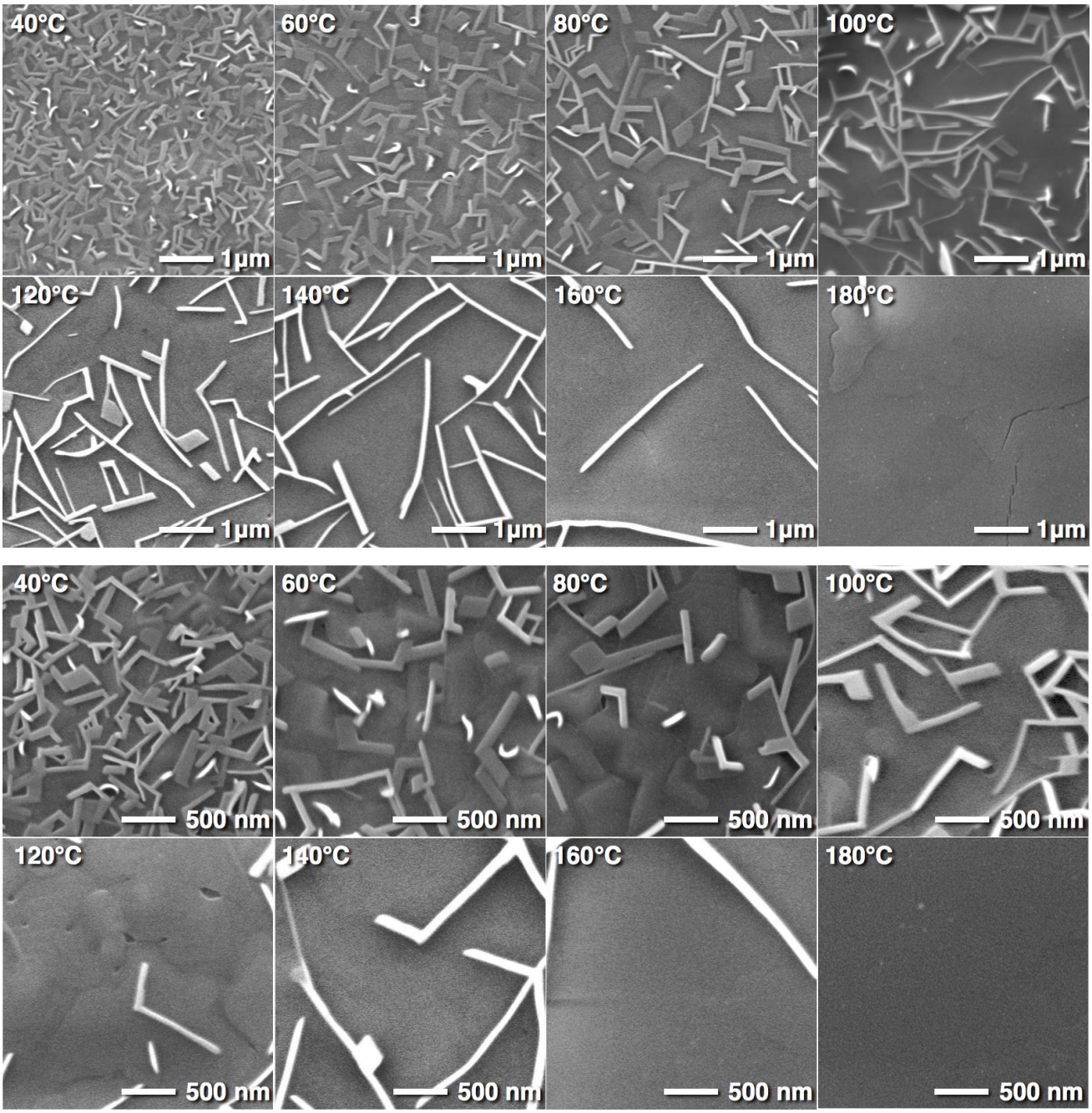

Fig. S4 SEM image of thin film surface based on **BP2Tz(in)**.

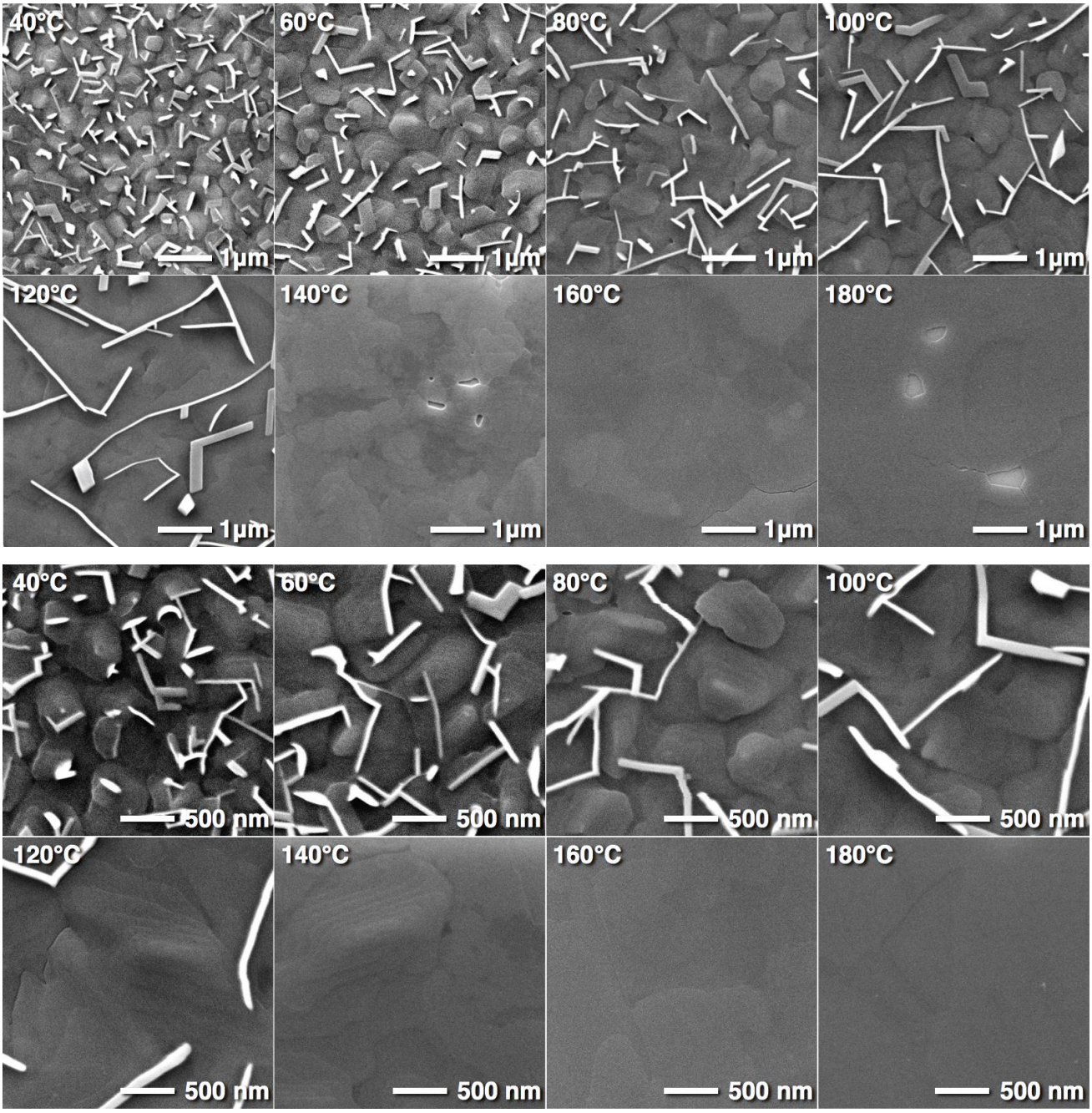

Figure S5. SEM image of thin film surface based on **BP2Tz(out)**.

Fabrication of OTFTs on TTC-SiO_2 substrate

BP2Tz transistors were fabricated on an n-type highly doped silicon substrate with a 300 nm-thick SiO_2 layer as a gate electrode and a dielectric layer. The substrates were cleaned by ultrasonication in acetone, ethanol, and 2-propanol followed by O_2-plasma treatment. The substrate was subsequently modified by thermally deposited TTC with 9 nm in thickness. The BP2Tz thin film (30 nm) was deposited by a vacuum vapor deposition method. Thin film transistors were made by evaporating highly purified molecules under high vacuum (10^{-6} Torr). The thin film deposition rate was maintained at 0.1 Å/s, and the substrate was kept at room temperature. Au was deposited onto the thin films by vacuum vapor deposition with a shadow mask. The channel length and the width were 100 μm and 12000 μm, respectively. The electrical characterization of thin film transistors were performed in the glove box under an inert Ar atmosphere by using a semiconductor parameter analyzer (Agilent Technology B1500A) and a CCD camera through an optical microscope.

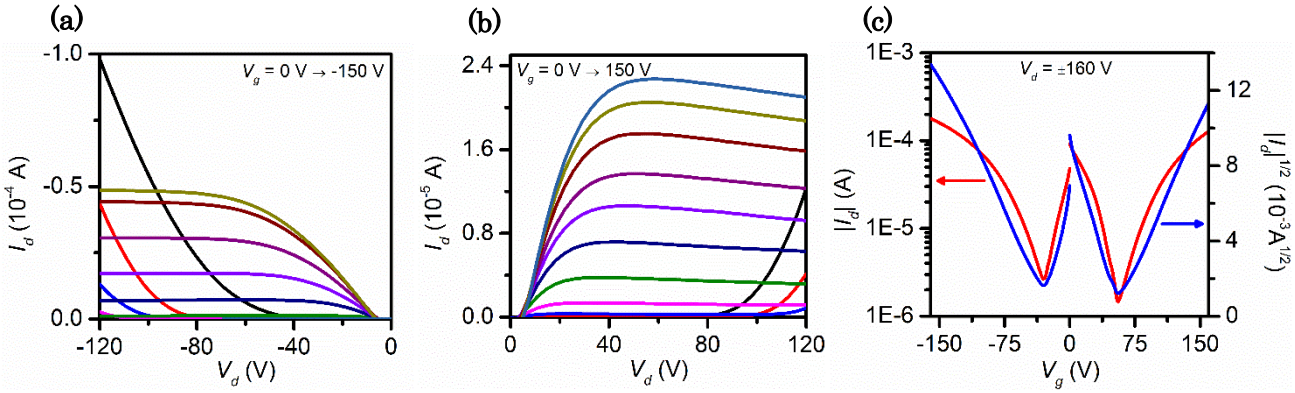

Fig. S6 Output (a, b) and transfer (c) characteristics of **BP2Tz(in)**-based OTFT with tetratetracontane (TTC)/SiO_2/Si substrate. Carrier mobility: μ_h = 0.012 cm^2 V^{-1} s^{-1}; μ_e = 0.015 cm^2 V^{-1} s^{-1}

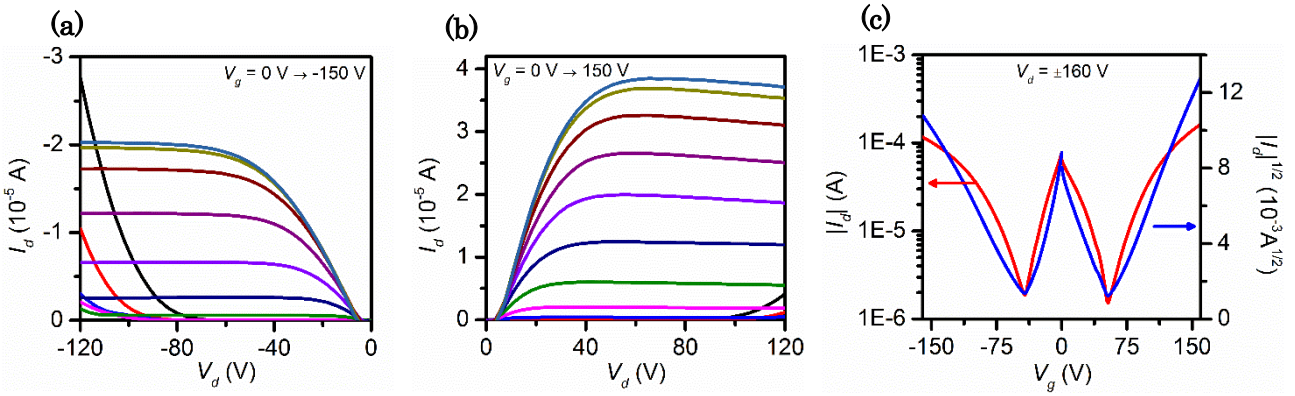

Fig. S7 Output (a, b) and transfer (c) characteristics of **BP2Tz(out)**-based OTFT with TTC/SiO_2/Si substrate. Carrier mobility: μ_h = 0.01 cm^2 V^{-1} s^{-1}; μ_e = 0.015 cm^2 V^{-1} s^{-1}

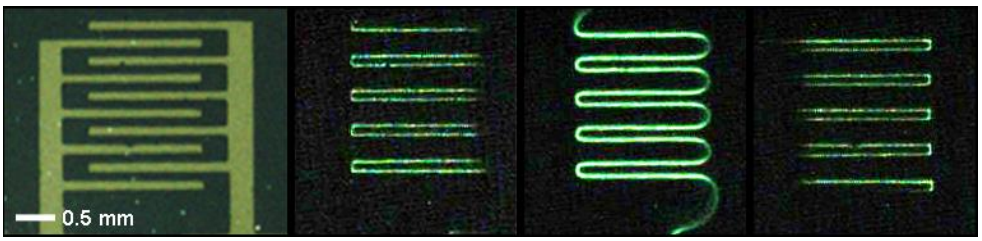

Fig. S8 Light emission of an ambipolar OTFT based on **BP2Tz(out)**.

References

[1] Gaussian 09, Revision C.01, Frisch, M. J.; Trucks, G. W.; Schlegel, H. B.; Scuseria, G. E.; Robb, M. A.; Cheeseman, J. R.; Scalmani, G.; Barone, V.; Mennucci, B.; Petersson, G. A.; Nakatsuji, H.; Caricato, M.; Li, X.; Hratchian, H. P.; Izmaylov, A. F.; Bloino, J.; Zheng, G.; Sonnenberg, J. L.; Hada, M.; Ehara, M.; Toyota, K.; Fukuda, R.; Hasegawa, J.; Ishida, M.; Nakajima, T.; Honda, Y.; Kitao, O.; Nakai, H.; Vreven, T.; Montgomery, J. A.; Peralta, Jr., J. E.; Ogliaro, F.; Bearpark, M.; Heyd, J. J.; Brothers, E.; Kudin, K. N.; Staroverov, V. N.; Keith, T.; Kobayashi, R.; Normand, J.; Raghavachari, K.; Rendell, A.; Burant, J. C.; Iyengar, S. S.; Tomasi, J.; Cossi, M.; Rega, N.; Millam, J. M.; Klene, M.; Knox, J. E.; Cross, J. B.; Bakken, V.; Adamo, C.; Jaramillo, J.; Gomperts, R.; Stratmann, R. E.; Yazyev, O.; Austin, A. J.; Cammi, R.; Pomelli, C.; Ochterski, J. W.; Martin, R. L.; Morokuma, K.; Zakrzewski, V. G.; Voth, G. A.; Salvador, P.; Dannenberg, J. J.; Dapprich, S.; Daniels, A. D.; Farkas, O.; Foresman, J. B.; Ortiz, J. V.; Cioslowski, J.; and Fox, D. J., Gaussian, Inc., Wallingford CT, 2010.